Egypt. J. Chem. **Vol. 65,** No. SI:13, pp. 1121 - 1136 (2022)

Egyptian Journal of Chemistry

http://ejchem.journals.ekb.eg/

Synthesis, Biological Evaluation and Molecular Docking Studies of Newly Synthesized 4- Amino Quinazoline Derivatives as Potential Multitarget Anticancer Agents.

Eman G. Said [a], Mohammed T. Elsaadi [a,b], Asmaa A. Mohammed [a*], Noha H. Amin [a]

[a] *Department* of Medicinal Chemistry, Faculty of Pharmacy, Beni-Suef University, Beni-Suef 62514, Egypt

[b] Department of *Medicinal* Chemistry, Faculty of Pharmacy, Sinai University, Kantra, Egypt. *and Fisheries, Cairo, Egypt.*

Abstract

A series of 4-aminoquinazoline linked to cyanopyrimidine derivatives (6a-c and 7a-f) was designed, synthesized with good yields and screened at National Cancer Institute (NCI)-disease oriented anticancer screen protocol against nine panel of cancer cell lines. Comprehensively, the structures of the synthesized compounds were confirmed by different spectroscopic methods like 1H-NMR, 13C-NMR and HRMS. Moreover, the most active compound 7a was selected for invitro enzyme inhibitory activities against epidermal growth factor receptor, cyclin dependent kinase-2 and TS enzymes, it exhibited good EGFR, CDK-2 and TS inhibition activity with IC50values of 0.313±0.019, 0.485±0.025 and 32.57±1.98 µM, respectively, in comparison to references with IC50 value of 0.03±0.002, 0.289±0.015 and 8.099±0.49µM, respectively. Cell cycle analysis and apoptosis were evaluated on three different cancerous cells; UO-31, MCF7 and IGROV-1. Finally, the molecular modelling for compound 7a inside the ATP binding site of epidermal growth factor receptor and cyclin dependent kinase-2 enzymes was performed to predict the binding mode to the active site of these enzymes using lapatinib and ribociclib as standards respectively. Our research found that quinazoline-containing cyanopyrimidine derivatives were promising cytotoxic agents for further study.

Keywords: *Amino quinazolines; Multitarget antitumor; Molecular Docking; apoptosis*

1. Introduction

Cancer has been a major cause of worldwide health concerns that resulted in complicated medical conditions and everyday increasingly death records. Although there are many anticancer drugs, cancer treatment still forms a great challenge to medical scientists, mainly due to development of resistance against effective anticancer agents [1,2]. This drug resistance may be due to several factors like drug inactivation, reduced drug uptake, excessive drug efflux, DNA damage repair, target alterations or epithelial-mesenchymal transition (EMT) [3-6]. Interestingly, combination therapy has proved to be one of the clinical protocols used to get over resistance against anticancer agents [7]. Unfortunately, combination therapy is highly expensive and may result in drug-drug interactions [8]. Due to the multifactor nature of cancer, multitarget anticancer treatment has proven to be highly effective in preclinical and clinical studies [9-12]. Also, molecular-targeted therapy has emerged due to low toxicity and high selectivity compared to traditional drugs, since the best choice to overcome cancer resistance is to use hybrid drugs that attack multiple targets [13,14]. Hybrid drugs are chemical entities with two or more structural domains having variable biological activities [15,16], there are many literature review revealed that hybrid molecules have antiprliferative activities [17-19]. The epidermal growth factor receptor (EGFR) is a subtype of tyrosine kinase that plays an important role in cell growth regulation, proliferation, differentiation, metastasis and survival [20,21]. EGFR is overexpressed in different tumors including lung, brain, colon, bladder and ovarian tumors [22]. Therefore, EGFR tyrosine kinase represents an attractive target for the development of novel anticancer agents [23,24] Many research articles reported that certain substituted quinazolines (gefitinib, erlotinib and lapatinib) acted as the first line of inhibitors of EGFR [25-27] (Fig. 1).

*Corresponding author e-mail: Asmaa011134@pharm.bsu.edu.eg; dr.asmaa99@yahoo.com; (Asmaa abdelhamied Mohammed).
Receive Date: 13 July 2022, **Accept Date:** 31 October 2022, **First Publish Date:** 31 October 2022
DOI: 10.21608/EJCHEM.2022.150145.6506

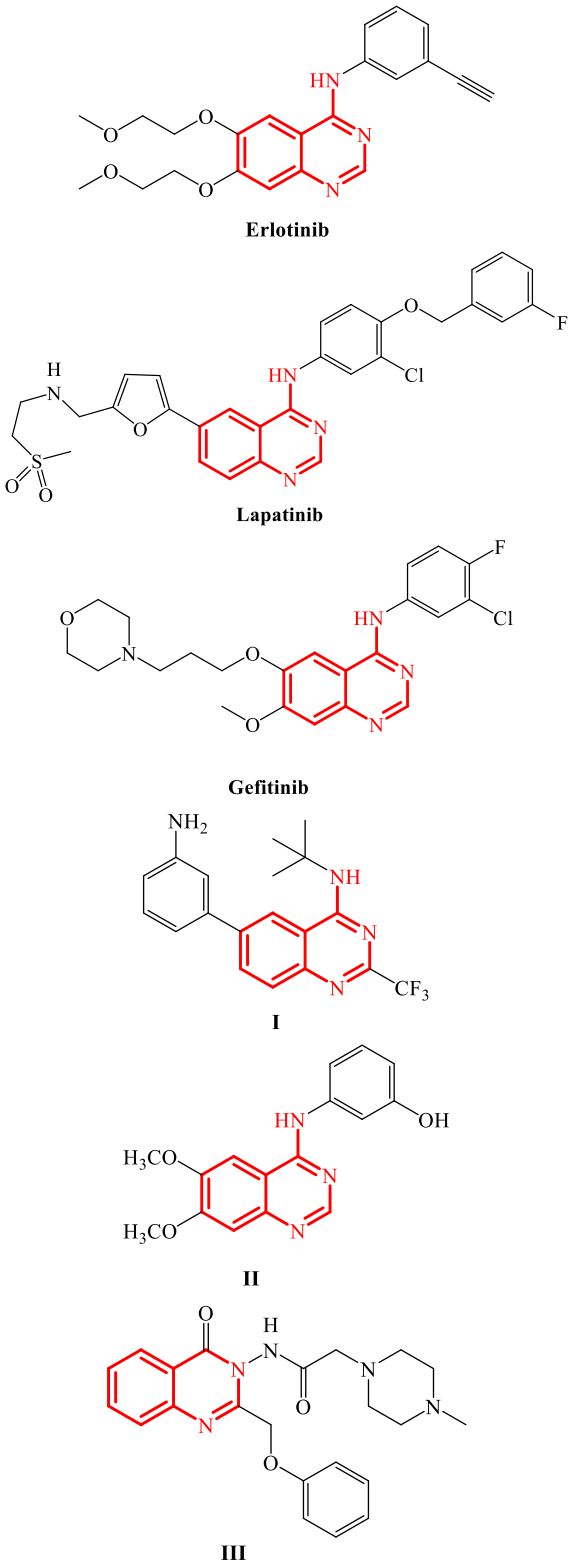

Fig. 1. Examples of anticancer quinazolines with EGFR and CDK-2 inhibitory properties.

Cyclin-dependent kinases (CDKs) are another type of enzymes that are responsible for protein phosphorylation necessary for cell division, differentiation and death. Regulation of cell cycle and transcription are controlled by CDK enzymes, while deregulation of cell cycle and transcription can lead to some diseases like cancer and neurodegenerative diseases [28-30]. It was reported that substituted quinazolines exhibited CDK-2 inhibitory activity exemplified by compounds I, II and III [31-33] (Fig. 1). Another strategy adapted in anticancer chemotherapy is to target thymidylate synthase enzyme (TS or Thy A), that is both a regulatory and catalytic protein that catalyze the methylation reaction of 2'-eoxyuridine-5'- monophosphate (dUMP) to 2'deoxythymidine-5'-monophosphate (dTMP) [34]. Collectively, thymidylate depletion, DNA damage, and induction of apoptosis can be accomplished by inhibition of TS [35-37]. Unfortunately, EGFR or CDK-2 tyrosine kinases inhibitors may develop resistance in most cases [38,39]. Also, the role of TS in the development of tumor resistance to fluoropyrimidines has been studied [40], where literature survey has shown that increased levels of TS protein may be associated with fluorouracil(5-FU) resistance [41]. Thus, multitargated strategies that may include TS expression have proved to be promising choice [42]. Chemical structure of the ligands, key pharmacophoric moieties and targeted enzymes should be well specifiesto obtain efficient drugs. Also, the appropriate cleavable linker that cleavages and releases active drugs at the site of action should be highlighted to avoid systemic toxicity [43,44]. Corresponding to this investigation, we designed quinazoline nucleus linked to pyrimidine nucleus through a cleavable aliphatic chain. In addition, literature survey showed that many effective anticancer agents were derived from the dihydropyrimidine/ tetrahydropyrimidine nuclei linked by an aliphatic linker to quinazoline iso steres; naphthalene and benzo thiazole [45,46] (fig.2)

Search survey revealed that the *invitro* antitumor activity of compound VI has higher cytotoxic activity against many tumors such as hepatocellular carcinoma and melanoma cell lines more than dasatinib [47]. On continuation of our searches to design and synthesize new multitarget anti-cancer agents [46], a **pharmacophoric** approach was adopted in which the quinazoline and substituted dihydropyrimidine moieties were linked in one structure hoping to synergize the anticancer activity of both groups. The synthesized compounds were screened for growth inhibition cell lines in NCI. The most active compound 7a was also screened for kinases enzymes (EGFR, CDK and TS) inhibition activities invitro. Cell cycle analysis and apoptosis were performed on this compound to establish the mechanism of cell death. In addition, molecular docking was employed on compound 7a to predict plausible protein-ligand interactions at molecular level.

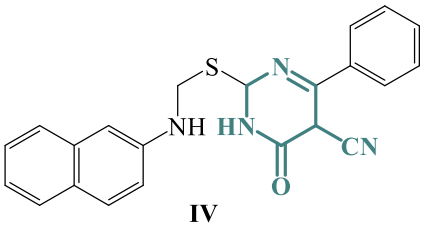

IV

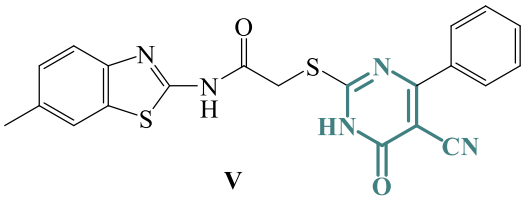

V

Fig.2. Chemical structures of reported dihydro pyrimidine having anticancer activity.

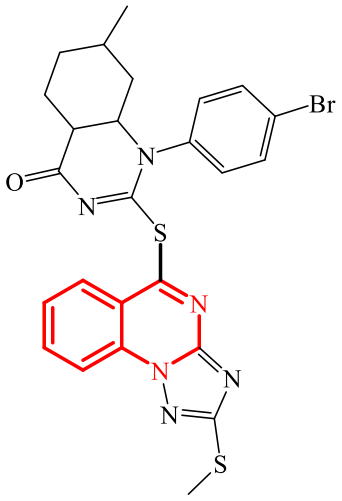

VI

2. Materials and methods

2.1. Experimental section

All the starting materials were purchased from Sigma-Aldrich and used without further purification. All the reactions were followed by TLC using silica gel F254 plates (Merck), using hexane/ ethyl acetate as an eluting system and were visualized by UV-lamp. Melting points were uncorrected and were carried out by open capillary tube method using IA 9100MK-Digital Melting Point Apparatus. IR spetra were made on Bruker Vector 22 (Germany) or J a s c o FTIR Plus 460 (Japan). Proton magnetic resonance ^{1}H-NMR (400 MHz) and carbon magnetic resonance ^{13}C-NMR (100 MHz) spectra were recorded on a Varian Mercury VX- 400 NMR spectrometer, Faculty of Pharmacy, Beni-Suef University. The spectra were run at 400 MHz spectrometers in deuterated chloroform or dimethyl sulfoxide(DMSO-d_6) using tetra methylsilane as internal standard. Chemical shifts were reported as ppm downfield from tetramethylsilane. Spin multiplicities were described as s (singlet), d (doublet), t (triplet), q (quartet), or m (multiplet). Coupling constants were reported in hertz (Hz). Chemical shifts were quoted in δ units and were related to that of the solvents. As for the proton magnetic resonance, D_2O was carried out for NH and OH exchangeable protons. Mass spectra were recorded on Finnigan MAT, SSQ 7000 (70 eV) mass spectrometer, Al-Azhar university, Giza, Egypt. Elemental Microanalyses were carried out at the Micro analytical center, Cairo University, Giza, Egypt and at the regional center for Mycology and Biotechnology, Al-A zhar university, Giza, Egypt. All the compounds were named according to the IUPAC system using Chem Draw Ultra 7.01 software programme.

Compounds 2,3,4 and 5a-c were previously prepared and reported [48-50].

General procedure for synthesis compounds 6a-c.

A mixture of 2-chloro-N-(quinazoline-4-yl) acetohydrazide4 (10mmol, 1.8 g) and the appropriate derivatives 5 a-c (10mmol) was refluxed in dry acetone (20 mL) for 10hrs in presence of anhydrous potassium carbonate (10mmol, 2.0 g). The separated solid was filtered, washed with water, dried and crystallized from ethanol to obtain 6a-c.

2-((5-Cyano--6oxo-4-phenyl-1,6-dihydropyrimidin-2-yl)thio)-N-(quinazoline-4-yl)acetohydrazide (6a).

Buff powder (78%); m p: 206-207°C. IR (K Br): 3384 (NHs); 3177 (CH aromatic); 2950 (CH aliphatic); 2200 (C≡N); 1675 (COs); 1609 (C=N), 1466 (C=C). ^{1}H-NMR (DMSO-d_6): δ 3.87 (s, 2H, CH_2), 7.25 (t, *J* = 8 Hz, 3H, phenyl H-3, H-4& H-5), 7.28 (s, 1H, NH, exch. D_2O), 7.51 (d, *J* = 8 Hz, 2H, phenyl H-2 & H-6), 7.55 (s, 1H, NH, exch.D_2O), 7.66 (t, *J* = 8 Hz, 1H, quinazoline H-6), 7.68 (d, *J* = 8 Hz, 1H, quinazoline H-5), 7.82 (t, *J* = 8 Hz, 1H, quinazoline H-7), 7.84 (d, *J* = 8 Hz, 1H, quinazoline H-8), 8.11 (s, 1H, quinazolineH-2), 8.23 (s, 1H, NH, exch. D_2O). ^{13}C- NMR (DMSO-d_6) δ 39.2, 93.4, 115.9, 120.2, 125.9, 127.4, 128.5, 129.4, 134.8, 135.7, 139.5, 145.8, 148.9, 154.01, 158.1, 161.2, 164.5, 168.9, 171.0. MS, m/z: 429 (M+; 18.57 %); 316 (100%). Anal. Calcd. for $C_{21}H_{15}N_7O_2S$: C, 58.73; H, 3.52; N, 22.83 Found: C, 58.91; H, 3.67; N, 23.09.

2-((5-Cyano--6oxo-4-hydroxyl–phenyl-1,6-dihydropyrimidin-2-yl)thio)-N'-(quinazoline-4-yl)acetohydrazide (6b).

Yellow powder (77%); m p: 205-206°C. IR (K Br): 3361 (br OH & NHs); 3157 (CH aromatic); 2930 (CH aliphatic); 2206 (C≡N); 1681 (COs); 1611 (C=N), 1466 (C=C). ^{1}H-NMR (DMSO-d_6): δ 3.90 (s, 2H, CH_2), 7.05 (d, *J* = 8 Hz, 2H, phenyl H-3& H-5), 7.19 (s, 2H, NHs, exch. D_2O), 7.51 (d, *J* = 8 Hz, 2H, phenyl H-2 & H-6), 7.67 (t, *J* = 8 Hz, 1H, quinazoline H-6), 7.69 (d, *J* = 8 Hz, 1H, quinazoline H-5), 7.82 (t, *J* = 8 Hz, 1H, quinazoline H-7), 7.84 (d, *J* = 8 Hz, 1H, quinazoline H-8), 8.11 (s, 2H, quinazoline H-2 & NH, exch. D_2O), 8.37 (s, 1H, OH, exch. D_2O). ^{13}C- NMR (DMSO-d_6): δ 39.3, 95.0, 115.2, 120.1, 122.8, 123.1, 127.1, 130.3, 131.9, 134.8, 136.4, 141.2, 144.2, 145.8, 148.7, 154.9, 160.6, 167.3, 171.9. MS, m/z: 445 (M+; 19.57%); 363 (100%). Anal. Calcd. for $C_{21}H_{15}N_7O_3S$: C, 56.62; H, 3.39; N, 22.01 Found: C, 56.86; H, 3.41; N, 22.24.

2-((5-Cyano-6oxo-4-chloro-phenyl-1,6-dihydropyrimidin-2-yl)thio)-*N'*-(quinazolin-4-yl)acetohydrazide (6c).

Orange powder (73%); m p: 217-219°C. IR (K Br): 3333 (NHs); 3156 (CH aromatic); 2925 (CH aliphatic); 2206 (C≡N); 1660 (COs); 1612 (C=N), 1497 (C=C); 770 (C-Cl). ^{1}H-NMR (DMSO-d_6): δ 3.18 (s, 2H, CH_2), 5.89 (s, 1H, NH, exch. D_2O), 7.27 (d, *J* = 8 Hz, 2H, phenyl H-3 & H-5), 7.48 (d, *J* = 8 Hz, 2H, phenyl H-2 & H-6), 7.65 (t, *J* = 8 Hz, 1H, quinazoline H-6), 7.67 (d, *J* = 8 Hz, 1H, quinazoline H-5), 7.78 (t, *J* = 8 Hz, 1H, quinazoline H-7), 7.82 (d, *J* = 8 Hz, 1H, quinazoline H-8), 7.89 (s, 1H, NH, exch. D_2O), 8.13 (s, 2H, quinazoline H-2 & 1NH, exch. D_2O). ^{13}C-NMR (DMSO-d_6): δ 35.5, 94.1, 118.1, 121. 6, 123.3, 129.4, 130.6, 131.6, 132.6, 134.4, 139.2, 145.8, 147.4, 148.9, 149.3, 154.0, 162.7, 165.8, 171.0. MS, m/z: 463 (M+; 7.76%); 317 (100%). Anal. Calcd. for $C_{21}H_{14}ClN_7O_2S$: C, 54.37; H, 3.04; N, 21.14 Found: C, 54.59; H, 3.21; N, 21.39

General procedure for synthesis of compounds (7a-f).

Methyl iodide/benzyl chloride (10 mmol) was added to a mixture of 6a-c (10 mmol) and anhydrous potassium carbonate (15 mmol, 1.8 g) in absolute ethanol (20 mL). The reaction mixture was heated under reflux for about 7hrs, evaporate to dryness. Then the residue was crystallized from ethanol.

2-((5-cyano-1-methyl-6-oxo-4-phenyl-1,6-dihydropyrimidin-2-yl)thio)-*N'*-(quinazolin-4-yl)acetohydrazide (7a).

Off-white powder (74%); m p: 204-205°C. IR (K Br): 3359 (NHs); 3157 (CH aromatic); 2910 (CH aliphatic); 2205 (C≡N); 1680 (COs); 1613 (C=N), 1467 (C=C). ^{1}H-NMR (DMSO-d_6): δ 2.35 (s, 1H, NH, exch. D_2O), 3.51 (s, 3H, CH_3), 3.77 (s, 2H, CH_2), 7.19 (t, *J* = 8 Hz, 3H, phenyl H3, H-4 & H-5), 7.31(d, *J* = 8 Hz, 2H, phenyl H-2 & H-6), 7.67 (t, *J* = 8 Hz, 1H, quinazoline H-6), 7.69 (d, *J* = 8 Hz, 1H, quinazoline H-5), 7.78 (t, *J* = 8 Hz, 1H, quinazoline H-7), 7.80 (d, *J* = 8 Hz, 1H, quinazoline H-8), 8.08 (s, 1H, NH, exch. D_2O), 8.39 (s, 1H, quinazoline H-2). ^{13}C- NMR (DMSO-d_6): δ 25.7, 33.2, 94.2, 115.9, 123.3, 128.4, 129.8, 130.5, 131.2, 134.6, 139.5, 142.3, 145.7, 147.8, 150.9, 156.1, 158.2, 163.7, 166.5, 175.8. MS, m/z: 443 (M+; 11.07%); 40.14 (100%). Anal. Calcd. for $C_{22}H_{17}N_7O_2S$: C, 59.58; H, 3.86; N, 22.11 Found: C, 59.67; H, 3.95; N, 22.35.

2-((5-Cyano-1-benzyl-6-oxo-4-phenyl-1,6-dihydropyrimidin-2-yl) thio)-N'-(quinazolin-4-yl)acetohydrazide (7b).

Brown powder (79%); m p: 211-213°C. IR (K Br): 3330 (NHs); 3050 (CH aromatic); 2942 (CH aliphatic); 2209 (C≡N); 1631 (COs); 1605 (C=N), 1404 (C=C). ^{1}H-NMR (DMSO-d_6): δ 3.74 (s, 2H, CH_2), 5.22 (s, 2H, benzyl CH_2), 7.29 (s, 1H, NH, exch. D_2O), 7.32 (t, *J* = 8 Hz, 3H, benzyl H-3, H-4 & H-5), 7.34 (d, *J* = 8 Hz, 2H, benzyl H-2 & H-6), 7.53 (t, *J* = 8 Hz, 3H, phenyl H-3, H-4 & H-5), 7.55 (d, *J* = 8 Hz, 2H, phenyl H-2 & H-6), 7.70 (t, *J* = 8 Hz, 1H, quinazoline H-6), 7.72 (d, *J* = 8 Hz, 1H, quinazoline H-8), 7.81 (t, *J* = 8 Hz, 1H, quinazoline H-7), 7.83 (d, *J* = 8 Hz, 1H, quinazoline H-5), , 8.18 (s, 1H, NH, exch. D_2O), 8.60 (s, 1H, quinazoline H-2). ^{13}C- NMR (DMSO-d_6): δ 35. 5, 49.3, 96.3, 114.9, 121.8, 122.1, 126.6, 128.1, 129.0, 130.6, 134.8, 137.0, 138.2, 145.8, 148.3, 150.9, 151.3, 155.9, 157.5, 159.6, 160.6, 161. 3, 168.5, 171.9. MS, m/z: 519 (M+; 9.43%); 42.98 (100%). Anal. Calcd. for $C_{28}H_{21}N_7O_2S$: C, 64.73; H, 4.07; N, 18.87 Found: C, 64.89; H, 4.23; N, 19.09.

2-((5-Cyano-1-methyl-6-oxo-4-hydroxylphenyl-1,6-dihydropyrimidin-2-yl)thio)-N'-(quinazolin-4-yl) acetohydrazide (7c)

Yellowish-orange powder (68%); m p: 203-204°C. IR (K Br): 3410 (OH); 3246 (NHs); 3130 (CH aromatic); 2948 (CH aliphatic); 2220 (C≡N); 1670 (COs); 1617 (C=N), 1454 (C=C). ^{1}H-NMR (DMSO-d_6): δ 3.51 (s, 3H, CH_3), 3.77 (s, 2H, CH_2), 7.28 (s, 1H, NH, exch. D_2O), 7.46 (d, *J* = 8 Hz, 2H, phenyl H-3 & H-5), 7.55 (d, *J* = 8 Hz, 2H, phenyl H-2 & H-6), 7.67 (t, *J* = 8 Hz, 1H, quinazoline H-6), 7.69 (d, *J* = 8 Hz, 1H, quinazoline H-5) 7.82 (t, *J* = 8 Hz, 1H, quinazoline H-7), 7.84 (d, *J* = 8 Hz, 1H, quinazoline H-8), 8.18 (s, 1H, NH, exch. D_2O), 8.40 (s, 2H, quinazoline H-2, OH, exch. D_2O). ^{13}C- NMR (DMSO-d_6): δ 28.8, 33.9, 97.3, 115.9, 120.1, 121. 6, 125.9, 127.4, 129.13, 130.2, 134.4, 139.5, 141.2, 143.7, 149.3, 154.0, 160.9, 163.2, 165. 7, 171.7.MS, m/z: 459 (M+; 9.06%); 40.43 100%). Anal. Calcd. for $C_{22}H_{17}N_7O_3S$: C, 57.51; H, 3.73; N, 21.34 Found: C, 57.77; H, 3.85; N, 21.08.

2-((5-Cyano-1-benzyl-6-oxo-4-hydroxylphenyl-1,6-dihydropyrimidin-2-yl)thio)-*N'*-(quinazolin-4-yl) acetohydrazide (7d)

Dark brown powder (65%); m p: 219-220°C. IR (K Br): 3421 (br OH); 3340 (NHs); 3134 (CH aromatic); 2912 (CH aliphatic); 2159 (C≡N); 1660 (COs); 1617 (C=N), 1468 (C=C). ^{1}H-NMR (DMSO-d_6): δ 3.74 (s, 2H, CH_2), 5.20 (s, 2H, benzyl CH_2), 7.30 (t, *J* = 8 Hz, 3H, benzyl H-3, H-4 & H-5), 7.32 (d, *J* = 8 Hz, 2H, benzyl H-2, H-6), 7.47 (d, *J* = 8 Hz, 2H, phenyl H3 & H-5), 7.55 (d, *J* = 8 Hz, 2H, phenyl H-2 & H-6), 7.70 (t, *J* = 8 Hz, 1H, quinazoline H-6), 7.72 (d, *J* = 8 Hz, 1H, quinazoline H-5), 7.83 (t, *J* = 8 Hz, 1H, quinazoline H-7), 7.85 (d, *J* = 8 Hz, 1H, quinazoline H-8), 8.16 (s, 1H, NH, exch. D_2O), 8.18 (s, 1H, NH, exch. D_2O), 8.60 (s, 2H, quinazoline H-2 , OH, exch. D_2O). ^{13}C- NMR (DMSO-d_6): δ 31.96, 48.98, 94.73, 115.8, 117.8, 120.3, 121.6, 121.8, 126.6, 127.9, 129.0, 130.1, 130.6, 134.8, 136.9, 139.77, 143.9, 148.3, 151.3, 155.8, 160.6, 164,7, 169.1, 171.0. MS, m/z: 535 (M+; 29.87%); 207.64 (100%). Anal. Calcd. for $C_{28}H_{21}N_7O_3S$: C, 62.79; H, 3.95; N, 18.31 Found: C, 62.61; H, 4.12; N, 18.45.

2-((5-Cyano-1-methyl-6-oxo-4-chlorophenyl-1,6-dihydropyrimidin—2-yl)thio)-*N'*-(quinazolin-4-yl) acetohydrazide (7e)

Pale buff powder (72%); m p: 199-200°C. IR (K Br): 3328 (NHs); 3066 (CH aromatic); 2949 (CH aliphatic); 2206 (C≡N); 1625 (COs); 1602 (C=N), 1402 (C=C); 768 (C-Cl). ^{1}H-NMR (DMSO-d_6): δ 3,51 (s, 3H, CH_3), 3.77 (s, 2H, CH_2), 7.31 (d, *J* = 8 Hz, 2H, phenyl H-3 & H-5), 7.46 (d, *J* = 8 Hz, 2H, phenyl H-2 & H-6), 7.60 (d, *J* = 8 Hz, 1H, quinazoline H-5), 7.76 (t, *J* = 8 Hz, 1H, quinazoline H-6), 7.78 (d, *J* = 8 Hz, 1H, quinazoline H-8), 7.87 (t, *J* = 8 Hz, 1H, quinazoline H-7), 8.09 (s, 1H, NH, exch. D_2O), 8.11 (s, 1H, NH, exch. D_2O), 8.38 (s, 1H, quinazoline H-2). ^{13}C- NMR (DMSO-d_6): δ 29.2, 34.5, 93.4, 111.5, 126. 6, 127.5, 128.1, 129.4, 131.9, 135.1, 137.3, 146.4, 148.3, 152.1, 157.2, 160.0, 162.2, 166.3, 167.9, 174.8. MS, m/z: 477 (M+; 13.24%); 426 (100%). Anal. Calcd. for $C_{22}H_{16}ClN_7O_2S$: C, 55.29; H, 3.37; N, 20.52 Found: C, 55.41; H, 3.50; N, 20.78

2-((5-Cyano-1-benzyl-6-oxo-4-chlorophenyl-1,6-dihydropyrimidin-2-yl)thio)-N'-(quinazolin-4-yl) acetohydrazide (7f)

66%); m p: 218-220°C. IR (K Br): 3316 (NHs); 3133 (CH aromatic); 2941 (CH aliphatic); 2207 (C≡N); 1629 (COs); 1603 (C=C), 1401 (C=N); 768 (C-Cl). ^{1}H-NMR (DMSO-d_6): δ 3,91 (s, 2H, CH_2), 5.89 (s, 2H, benzyl CH_2), 7.16 (s, 1H, NH, exch. D_2O), 7.27 (t, *J* = 8 Hz, 3H, benzyl H-3, H-4 & H-5), 7.34 (d, *J* = 8 Hz, 2H, benzyl H-2 & H-6), 7.51 (d, *J* = 8 Hz, 2H, phenyl H-3 & H-5), 7.55 (d, *J* = 8 Hz, 2H, phenyl H-2 & H-6), 7.67 (t, *J* = 8 Hz, 1H, quinazoline H-6), 7.69 (d, *J* = 8 Hz, 1H, quinazoline H-5), 7.76 (t, *J* = 8 Hz, 1H, quinazoline H-7), 7.78 (d, *J* = 8 Hz, 1H, quinazoline H-8), 8.11 (s, 1H, NH, exch. D_2O), 8.37 (s, 1H, quinazoline H-2). ^{13}C- NMR (DMSO-d_6): δ 35.7, 42.7, 93. 5, 116.5, 123.1, 126.3, 127.2, 127.5, 128.5, 130.6, 131.3, 134.1, 134. 8, 143.9, 145.5, 148.9, 149.2, 155.6, 157.9, 159.2, 161.2, 165.7, 169.9, 170.1. MS, m/z: 553 (M+; 24.24%); 148.53 (100%). Anal. Calcd. for $C_{28}H_{20}ClN_7O_2S$: C, 60.70; H, 3.64; N, 17.70 Found: C, 60.98; H, 3.72; N, 17.83

2.2. Biological evaluation

2.2.1. Preliminarily invitro cytotoxic screening

all the newly synthesized compounds were screened by the National Cancer Institute (NCI), USA against 60 human tumor cell lines derived from 9 types of cancer (non-small cell lung cancer, leukemia, CNS, colon, melanoma, ovarian, prostate, breast and renal cancer). Results of the screening showed different levels of cytotoxicity against different cell lines. The results were obtained as a mean graph one dose.The NCI screening procedures were described briefly, cell suspensions that were diluted according to the particular cell type and the expected target cell density (5000-40,000 cells per well based on cell growth characteristics) were added by pipet (100 µL) into 96-well microtiter plates. Inoculates were allowed a preincubation period of 24 h at 37 °C for stabilization. Dilutions at twice the intended test concentration were added at time zero in 100-µ L aliquots to the microtiter plate wells. Incubations lasted for 48 h in 5 % CO2 atmosphere and 100 % humidity. The cells were assayed by using the sulforhodamine B assay. A plate reader was used to read the optical densities, and a microcomputer processed the optical densities into the special concentration parameters defined later [51,52].

2.2.2. Invitro enzyme kinase activity

Further mechanistic studies were carried out for compound 7a at the confirmatory diagnostic unit using TECAN SPARK device (US) at VACSERA-EGYPT to investigate the possible mechanism of inhibition. EGFR/CDK-2 and thymidylate synthase assays were performed. The results were observed primarily as % inhibition at 10 µM. Secondly, determination of inhibitory concentration (IC_{50}) was indicated.

2.2.3. Cell cycle analysis and apoptosis inducing activity

Moreover, cell cycle analysis and apoptosis examinations were carried out using propidium iodide (PI) flow cytometry and Annexin V FITC Annexin-V/PI kit (Becton Dickenson, Franklin Lakes, NJ, USA) VACSERA-EGYPT on UO-31, MCF-7 and

IGROV-1[53]. Cells were incubated overnight at 37 °C and treated with 5 % CO2. After 48 h of incubation, pellets of cells were collected and centrifuged at 300 g for 5 min. For cell cycle analysis, cell pellets were placed in 70% ethanol on ice for 15 min. The collected pellets were treated with propidium iodide (PI) staining solution (50 µg/mL PI, 0.1 mg/mL RNase A and 0.05% Triton X-100) at room temperature for 1 h. Apoptosis detection was carried out by FITC Annexin-V/PI kit (Becton Dickenson, Franklin Lakes, NJ, USA) Samples' analyses were performed by fluorescence-activated cell sorting (FACS) with a Gallios flow cytometer (Beckman Coulter, Brea, CA, USA) within 1 h from the staining. Analysis of data was performed using Kaluza v1.2 (Beckman Coulter) [54].

2.3. Docking study

The crystal structures of EGFR kinase and CDK-2 were obtained from protein data bank using the following PDB IDs (1xkk and 1DI8), respectively. MOE 2019.03, Chemical Computing Group Inc., Montreal, Quebec, Canada was implemented in conducting the entire docking studies [55]. After download, refinement of EGFR and CDK-2 domain and removal of water chain, adding polar hydrogens and correcting charges according to AMBER12: EHT forcefield were done, then redocking of lapatinib and ribociclib, respectively, into the binding site was done to perform a verification process, after that the most active compound is also docked to the same binding site of EGFR tyrosine and CDK-2 kinase. Initially, a pose retrieval process was conducted for the co-crystalized coordinates of lapatinib and ribociclib in both EGFR and CDK-2, respectively. The coordinates of the best scoring docking pose of the native ligand were compared with its coordinates in the co-crystallized PDB file based on the binding mode and root mean square deviation (rmsd). Compound 7a, lapatinib and ribociclib as references were drawn by chemdraw. The titled compound 7a, lapatinib and ribociclib were docked into EGFR and CDK-2 active domain respectively then fifty poses of each compound were scored by initial rescoring methodology (London dG) and the final re-scoring methodology (GBVI/WSA dG) after placement using Triangle Matcher. MOE also was used to generate the required interaction images

3. Results and discussion

3.1. chemistry

The synthetic new target compounds **6a-c** and **7a-f** were depicted in Scheme1, Scheme 2 and Scheme 3.

Compounds **2, 3, 4** and **5a-c** were previously prepared and reported [44-46]. As shown in Scheme 1, 4-hydroxy quinazoline **1** was synthesized upon thereaction of equimolar amounts of anthranilic acid and formamide by fusion at 140ºC. The reaction involves elimination of water and proceeds via an *O*-amido benzamide intermediate. Then, compound **2** reacted with hydrazine hydrate by fusion in presence of zinc chloride as catalyst to afford 4-hydrazinequinazoline **3**. Then, compound **3** was acylated using acetic acid activated by N, N-carbonyl diimidiazole in dioxane to afford the chloroacetohydrazide **4** (Scheme 1).It was reported that compounds **5a-c** were prepared using equimolar amounts of ethylcyanoacetate, the appropriate benzaldehyde and thiourea in absolute ethanol in presence of potassium carbonate (Scheme 2).

Scheme 3 shows the synthesis of compounds **6a-c** obtained by reaction of equimoles of compounds **5a-c** with the acetyl chloride derivative **4** in dry acetone. IR spectra of **6a-c** supported the postulated structure due to theappearance of the characteristic bands of the cyano group at 2200, 2206, and 2206 cm^{-1}, respectively.^{1}H-NMR spectra of compounds **6a-c** revealed asinglet signal at 3.18-3.90 ppm attributed to $C\underline{H_2}S$ protons respectively. Mass spectrum of compound **6a-c** showed molecular ion peaks at m/z 429, 445 and 463, respectively, that was consistent with the molecular weight of the compounds. Compounds **6a-c** were *N*-alkylated with methyl iodide/ benzyl chloride in presence of anhydrous potassium carbonate as a catalyst in absolute ethanol to afford **7a-f**. Spectral analyses confirmed the suggested structures of compounds **7a-f**. H_1- NMR spectra of compounds **7a-f** showed singlet signals at (3.51, 3.51, 3.51, 5.22, 5.20 and 5.89 ppm) representing methyl/benzylic protons of compounds **7 a-f,** respectively (Scheme 3).

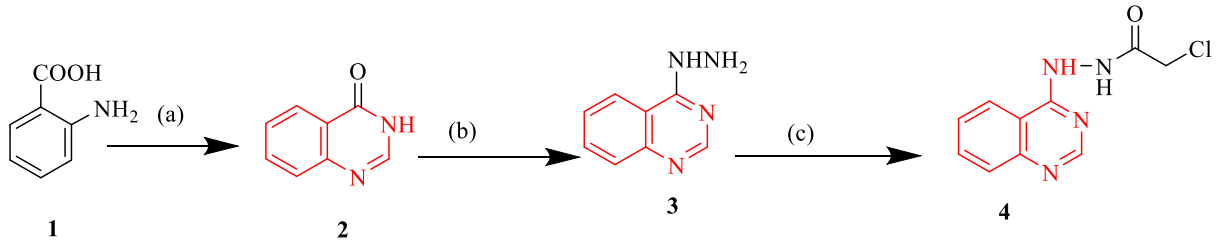

Scheme 1. Synthesis of compound **4**: (**a**) formamide, fusion, 2hr; (**b**) hydrazine hydrate, zinc (II) chloride, fusion, 8hr; (**c**) acetic acid, N, N-carbonyldiimidiazole, dioxane, heat,1 hr, stir,8hr, rt.

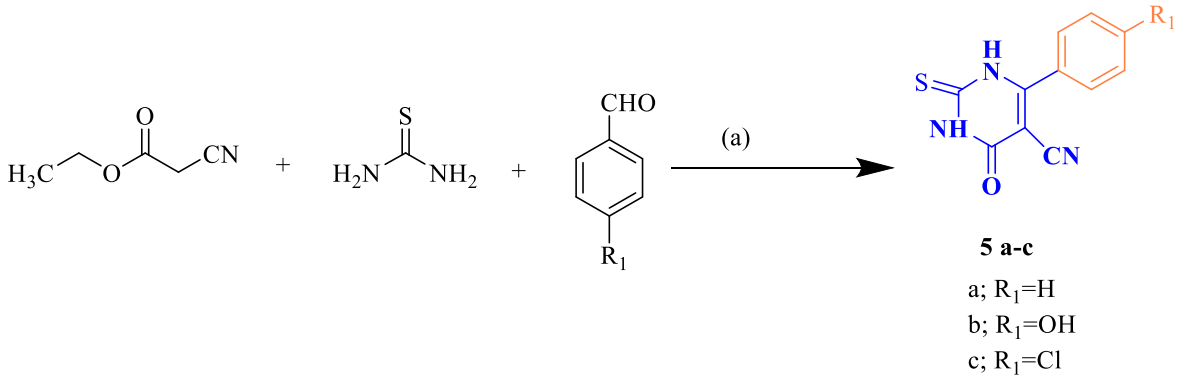

Scheme 2. Synthesis of compounds **5a-c:** (**a**) anhydrous potassium carbonate, absolute ethanol, reflux 10hr.

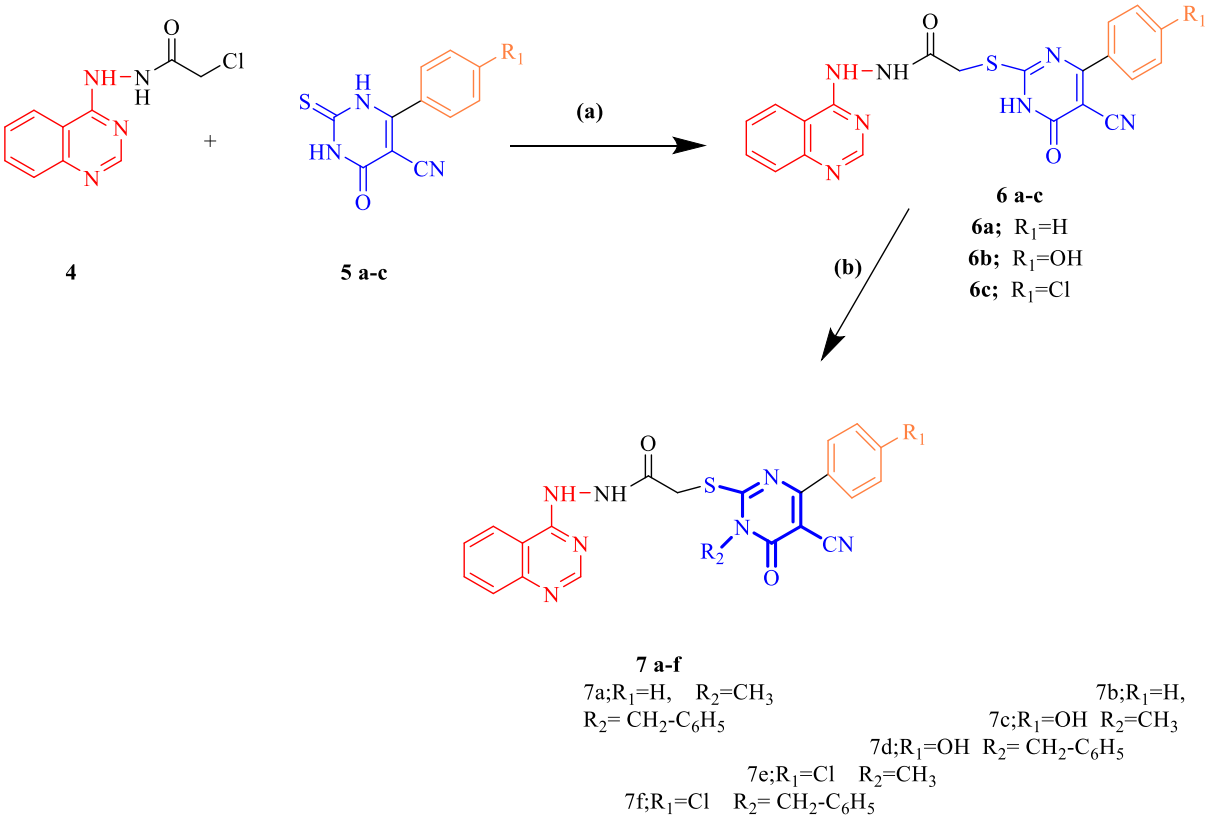

Scheme 3. Synthesis of compounds **6a-c** and **7a-f**: (**a**) dry acetone, anhydrous potassium carbonate, dry acetone, reflux 10hr; (**b**) methyl iodide/benzyl chloride, anhydrous potassium carbonate, absolute ethanol, relux,7 hr.

3.2. Biological evaluation

3.2.1. Invitro cytotoxic screening and structure activity relationship (SAR)

Results of the screening of the synthesized compounds by the National Cancer Institute (NCI), USA showed different levels of cytotoxicity against 60 human tumor cell lines derived from 9 types of cancer (non-small cell lung cancer, leukemia, CNS, colon, melanoma, ovarian, prostate, breast and renal cancer) with growth inhibition (GI) ranging from less than 4 and up to 25.25%. It was noticed that compound **7a** showed the broadest spectrum towards the tested tumor cell lines. Regarding selectivity to specific cell line, most of the synthesized compounds showed good activity against renal cancerous cell (UO-31).

Structure–activity correlation was based on the obtained results. It was noticed that the unsubstituted analogue **6a** possessed fair antiproliferative activity against most sensitive cell lines SKOV-3, PC-3, MCF7, IGROV-1, CAK-1, HOP-62 and UO-31 ranging GI% from 3.32 to 21.35, respectively. Besides, electron withdrawing groups like the chlorine atom as in compound **6c** slightly increased the anticancer activity relative to the unsubstituted derivative **6a** (GI % ranging from zero to 24.62 on the same cell lines, respectively). While the electron donating hydroxy group in compound **6b** decreased

the anticancer activity in comparison with the unsubstitutedone **6a** (GI% ranging from zero to 8.61 on the same cell lines, respectively). Regarding *N*-methyl substitution on pyrimidine ring, compound **7a** exhibited the widest spectrum of activity GI% ranging from zero to 22.11 on the most sensitive cell lines IGROV-1, PC-3, CAK-1, HOP-62, MCF-7, UO-31 and SKOV-3, respectively. On the otherhand N-aryl alkyl substitution as in **7b** diminishes cytotoxicity with GI% ranging from zero to 18.04 on the same cell lines. (Fig. 3) (Table 1).

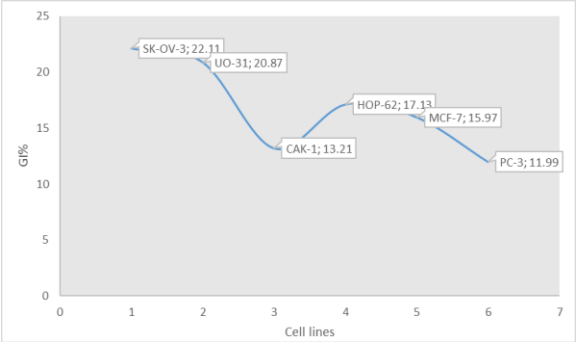

Fig. 3. Growth inhibitory activity % of compound 7a over the most sensitive cell lines.

3.2.2. Invitro enzyme inhibition assays.

Furthermore, *N*-methyl substituted pyrimidine derivative **7a** was chosen for screening its *invitro* inhibitory activities against EGFR, CDK-2 and TS enzymes (Table 2). Compound **7a** showed a high enzyme inhibition percentage towards EGFR and CDK-2 (87% and 81% respectively) when compared to lapatinib and ribociclib (93 % and 81.9 %, respectively). For TS enzyme, compound **7a**, showed an enzyme inhibition percentage = 63 % in comparison with 5-flurouracil (74 %). For further IC_{50} determination, compound **7a** showed moderate profile for EGFR, CDK-2 and TS enzyme inhibition (0.313±0.019, 0.485±0.025 and 32.57±1.98) relative to standard drugs (0.03±0.002, 0.289±0.015 and 8.099±0.49), respectively

3.2.3.mechanism of cell action

3.2.3.1 Cell cycle analysis

Cell cycle analysis was studied as pellets of cell were put in 70% ethanol on ice for 15 min. then the pellets were treated with propidium iodide (PI) staining solution (50 µg/mL PI, 0.1 mg/mL RNaseA and 0.05% Triton X-100) at room temperature for 1 h, where compound **7a** was introduced to induce apoptosis on UO-31, MCF-7 and IGROV-1 Cell lines. For UO-31 cell line, the percentages of cells markedly decreased from 54.16 % in G0/G1 phaseof the cell cycle to 11.89 % in G2/M phase (Table 3). For MCF-7 cell line, the percentages of cells markedly decreased from 42.91 % in G0/G1 phase of the cell cycle to 8.76 % in G2/M phase (Table 4). Finally, for IGROV-1 cell line, the percentages of cells markedly decreased from 38.93 % in G0/G1 phase of the cell cycle to 8.76 % in G2/M phase (Table 5) (Fig. 4 and 5).

Table 3. Cell cycle of compound **7a** on UO-31 cell line.

Table 1. Cytotoxicity of synthesized compounds **6a, 6b, 6c, 7a, 7b, 7c, 7d, 7e** and **7f** against selected cell lines

	Cell lines (GI%)						
Compound code	HOP-62	UO-31	CAK-1	SKOV-3	IGROV-1	MCF7	PC-3
6a	19.57	21.35	11.56	3.32	10.36	10.15	8.09
6b	4.87	8.61	7.31	zero	zero	4.22	zero
6c	13.88	24.62	13.96	zero	19.10	17.43	10.91
7a	17.13	20.87	13.21	22.11	zero	15.97	11.99
7b	7.11	18.04	9.68	2.56	0.63	9	zero
7c	10.88	23.38	10.87	zero	9.35	13.45	0.41
7d	3.08	20.62	11.08	zero	zero	8.85	3.91
7e	19.34	25.25	12.10	9.96	15.83	12.43	12.47
7f	1.45	19.65	9.66	zero	zero	6.30	8.06

Table 2. Multitargeted enzyme inhibitory activities of compound **7a** using lapatinib, ribociclib and 5-flurouracil as references showing their inhibition % at 10µg and enzyme inhibitory activity (IC_{50}).

Compound Code	**EGFR IC_{50} ug/ml**	**CDk-2 IC_{50} ug/ml**	**TS IC_{50} ug/ml**	**EGFR % Inhibition at 10 µg**	**CDk-2 % Inhibition at 10 µg**	**TS % Inhibition at 10 µg**
7a	**0.313**±0.019	**0.485**±0.025	**32.57**±1.98	**87**	**81**	**63**
Standard drug	**0.03**±0.002 [(a)]	**0.289**±0.015[(b)]	**8.099**±0.49[(c)]	**93[(a)]**	**81.9[(b)]**	**74[(c)]**

(a) lapatinib, (b) ribociclib, (c) 5-flurouracil

Table 3. Cell cycle of compound **7a** on UO-31 cell line.

Sample data	Results DNA content			
code	**%G0-G1**	**%S**	**%G2/M**	**Comment**
7a /UO-31	54.16	33.95	11.89	cell growth arrest@ S
Cont.UO-31	61.29	26.57	12.14	---

Table 4. Cell cycle of compound **7a** on MCF-7 cell line

Sample data	Results DNA content			
code	**% G0-G1**	**% S**	**%G2/M**	**Comment**
7a /MCF7	42.91	48.33	8.76	cell growth arrest@ S
Cont.MCF7	53.47	36.04	10.49	---

Table 5. Cell cycle of compound **7a** on IGROV-1 cell line

Sample data	Results DNA content			
code	**% G0-G1**	**% S**	**% G2/M**	**Comment**
7a /IGROV-1	38.93	52.31	8.76	cell growth arrest@ G1/S
Cont.IGROV-1	46.51	42.11	11.38	---

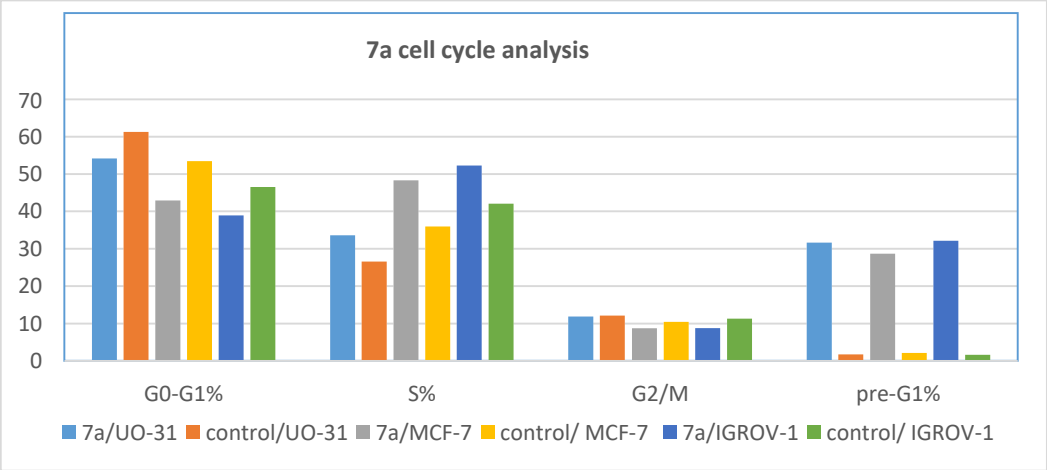

Fig. 4. Cell cycle analysis of compound 7a against UO-31, MCF-7 and IGROV-1 Cell lines.

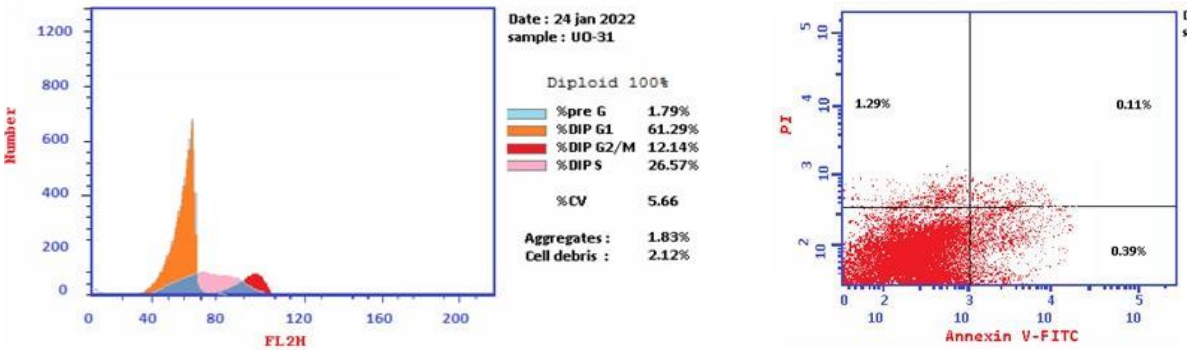

Control UO-31

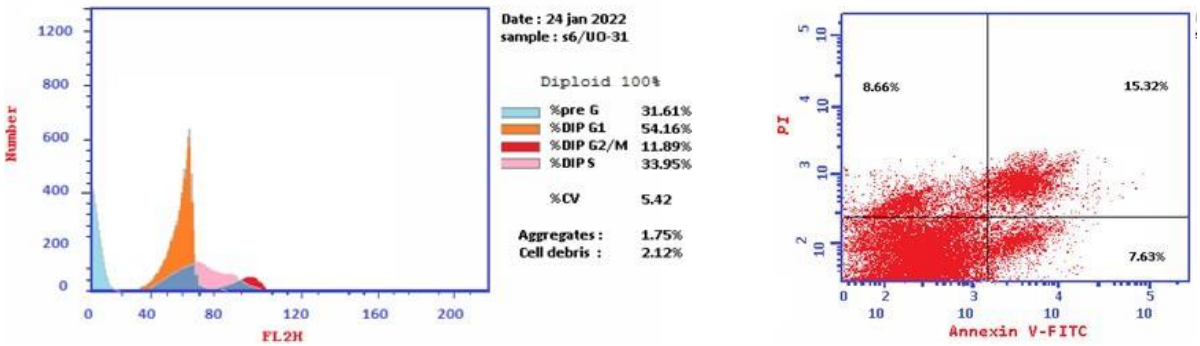

Compound 7a UO-31

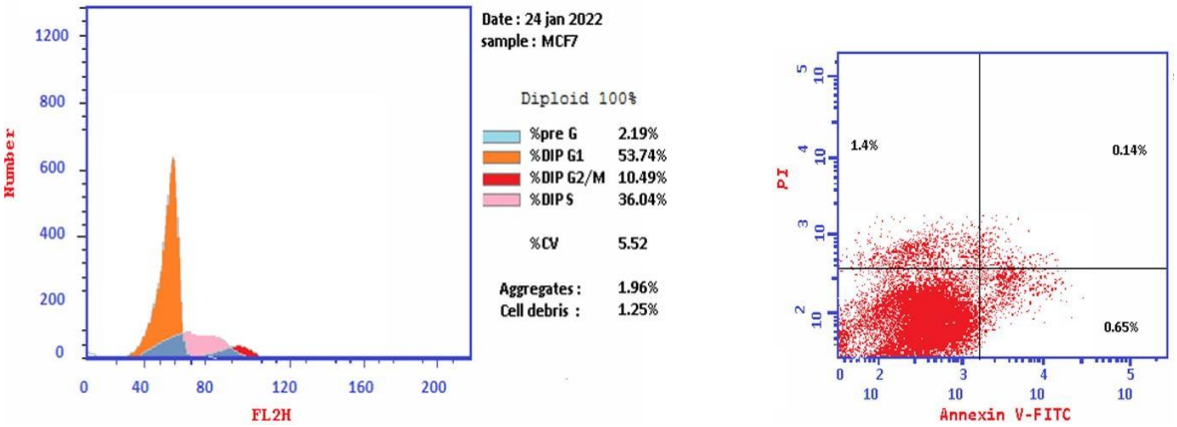

Control MCF-7

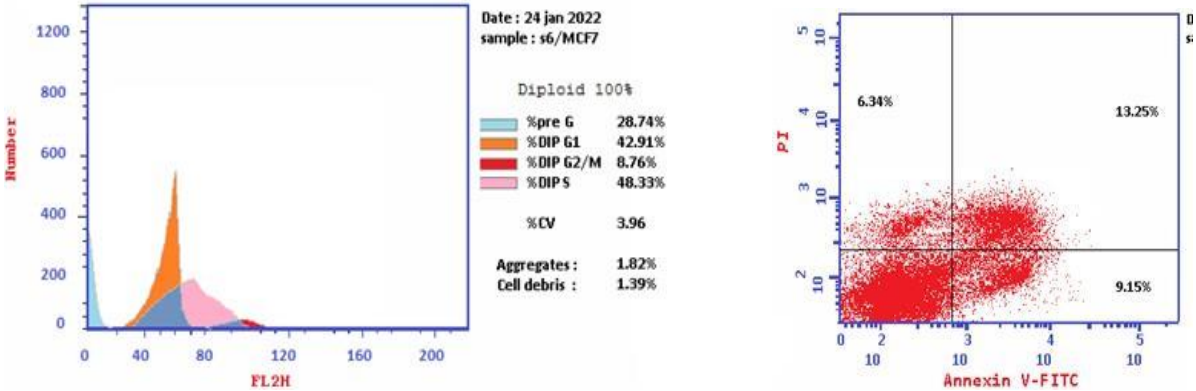

Compound 7a MCF-7

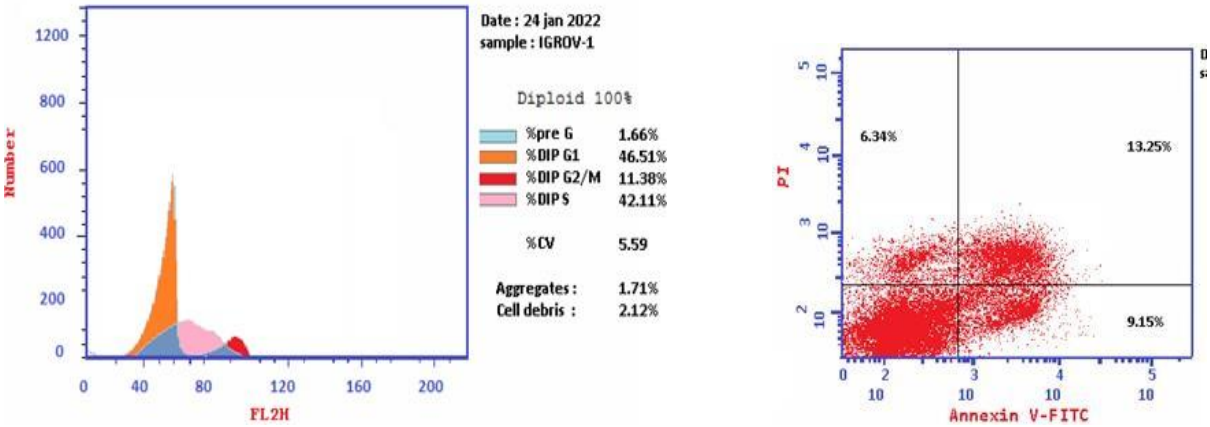

Control IGROV-1

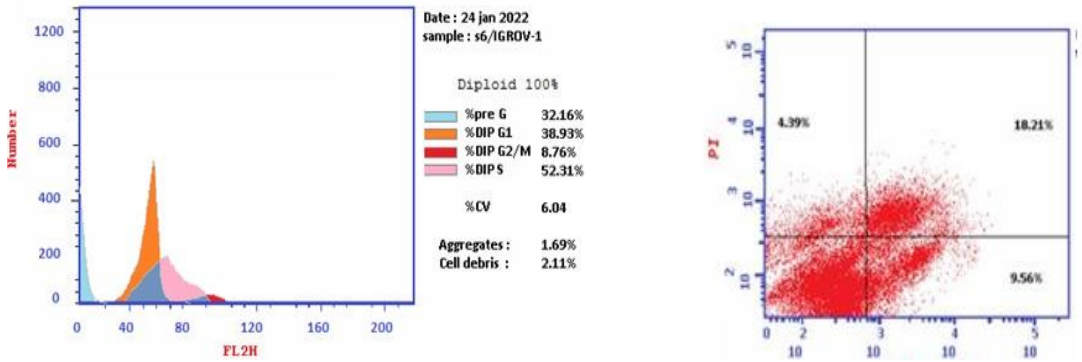

7a IGROV-1

Fig. 5. Representative dot plots of UO-31, MCF-7 and GROV-1 cells treated with compound 7a (10 µg) for 24 h and analyzed by flow cytometry after double staining of the cells with annexin-V FITC and PI

3.2.3.2. Cell apoptosis

Moreover, apoptotic cells percentages for compound **7a** against different cell lines were observed, Determination was carried out by V-FITC and PI staining (BectonDickenson, Franklin Lakes, NJ, USA). the analysis of sampleswere performed by fluorescence-activated cell sorting (FACS) with a Gallios flow cytometer (BeckmanCoulter, Brea, CA, USA) within 1 h from the staining. Analysis of data were performed by using Kaluza v1.2 (Beckman Coulter) Percentages increased from 1.29 % for control untreated UO-31 cells to be 8.66 % (Table 6), from 1.4 % for control untreated MCF-7 cells to be 6.34 % (Table 7) and from 0.93 for control untreated GROV-1 cellsto be 4.39 % (Table 8). From the above results, compound **7a** showed cell cycle arrest at G1, S phase and pre G1 apoptosis. Also compound **7a** showed a high apoptotic activity, since a significant increase in apoptotic/necrotic percentage was detected, if compared to the control untreated cells.

Table 6. Apoptosis of compound **7a** on UO-31 cell line.

Code	Apoptosis		Necrosis	
	Total	Early	Late	
7a /UO-31	31.61	7.63	15.32	8.66
Cont.UO-31	1.79	0.39	0.11	1.29

Table 7. Apoptosis of compound **7a** on MCF-7 cell line

Code	Apoptosis		Necrosis	
	Total	Early	Late	
7a/MCF7	28.74	9.15	13.25	6.34
Cont.MCF7	2.19	0.65	0.14	1.4

Table 8. Apoptosis of compound **7a** on IGROV-1 cell line

Code	Apoptosis		Necrosis	
	Total	Early	Late	
7a /IGROV-1	32.16	9.56	18.21	4.39
Cont.IGROV-1	1.66	0.44	0.29	0.93

Molecular docking study

The most active compound **7a** was further selected for molecular modeling studies to understand the binding mode and the origin of selectivity for both EGFR and CDK-2 enzymes using lapatinib and ribociclib as reference ligands, respectively. It showed both a good binding score and efficient interaction of the amino acids into the active site, suggesting that the antiproliferative activity may be due to their proposed mechanism of action as EGFR and CDK-2 inhibitors. The substituted 4-amino quinazoline**7a** showed interaction energy values (-14.7 Kcal/mol) for EGFR and (-15.1 Kcal/mol) for CDK-2, which were nearly close to those of lapatinib (-18.4 Kcal/mol) for EGFR and ribociclib (-15.3 kcal/mol) for CDK-2 (Table 9). From the docking study, corresponding toEGFR, NH group interacted with Asp800 via hydrogen bond, C=O group interacted with Cys797 via hydrogen bond and CN group interacted with Leu844 and Met793 via hydrogen bonds (Fig. 6). On the other hand, CDK-2 ligand interaction shows that carbonyl and amino groups of pyrimidine moiety interacted with Lys33 and Val18, respectively, via hydrogen bonds (Fig. 7). For EGFR and CDK-2, the hydrophobicity of the quinazoline**,** flouro phenyl moiety and pyrrolo pyrimidine were contributed in the hydrophobic interactions with different amino acid residues. Accordingly, docking study results of compound**7a** were well matched with the NCI screening and *in vitro* enzymatic inhibition results. Also, it was able to strongly interact with the receptors with many typesof interesting interactions. The docked results showed better CDK-2 interactionover EGFR enzyme.

Table 9. The docking scores and binding interactions of compound **7a** inside EGFR andCDK-2 active site.

EGFR				CDK-2			
CompoundNo.	**Binding Energy (Kcal/Mol)**	**No. H-Bond**	**H-Bond Details**	**Binding Energy (Kcal/Mol)**		**No. H-Bond**	**H-Bond Details**
Lapatinib	-18.4	4	Ser720 Asp855 Arg841 Lys745	**Ribociclib**	-15.3	4	Asp145 Lys33 lle10
7a	-14.7	4	Asp800 Cys797 Leu844 Met793	**7a**	-15.1	2	Lys33 Val18

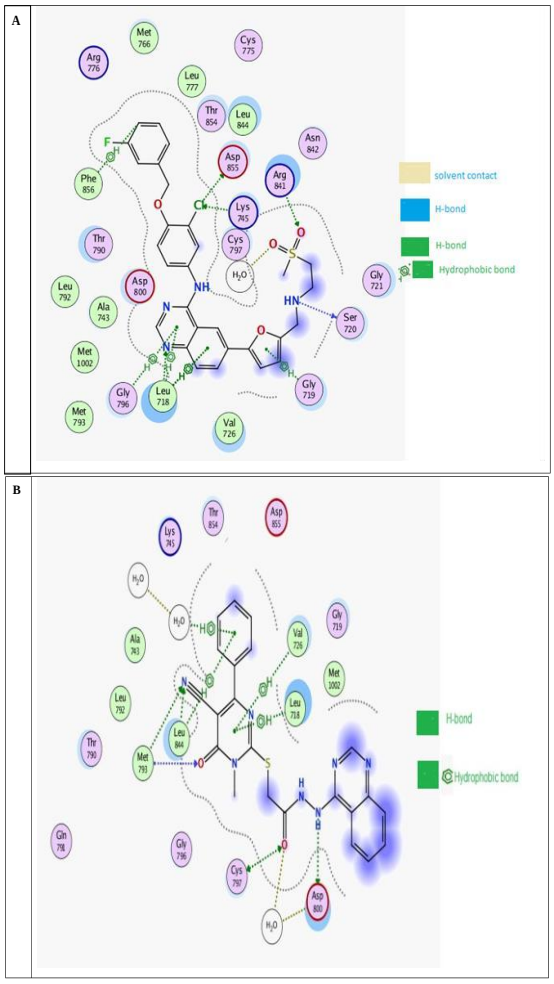

Fig.6. The 2D interaction diagram between the lapatinib (A) and compound 7a (B) towards EGFR enzyme

Conclusion

In this study, nine novel quinazolines derivatives **6a-c** and **7a-f** were synthesized through hybridization of the quinazoline nucleus with cyanopyrimidine derivatives. The new synthesized compounds were screened for their anticancer activities at NCI (USA). Most of the designed compounds demonstrated good antiproliferative activities against the renal cancer cell line (UO-31). The most active compound **7a** was screened for *in-vitro* enzyme inhibition against three enzymes (EGFR, CDK-2 and TS), It exhibited good EGFR, CDK-2 and TS inhibition activity with IC_{50}values of 0.313±0.019, 0.485±0.025 and 32.57±1.98 µM, respectively, in comparison to references with IC_{50} value of 0.03±0.002, 0.289±0.015 and 8.099±0.49µM, respectively .

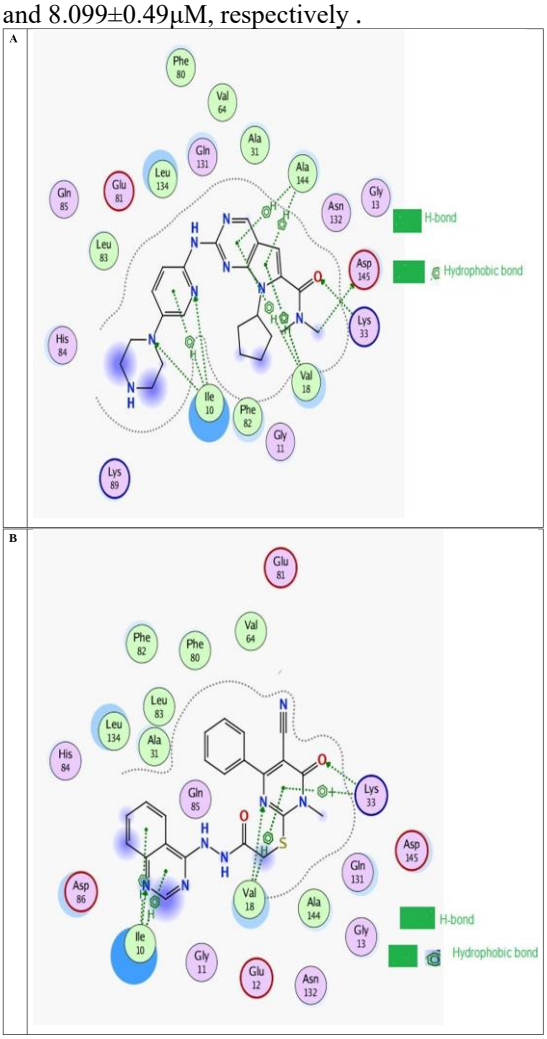

Fig.7. The 2D interaction diagram between the ribociclib (A) and compound 7a (B) towards CDK-2 enzyme

Moreover, cell cycle analysis and apoptosis were done, where compound **7a** showed valuable apoptotic activity towards tumor cells in UO-31, MCF-7 and IGROV-1 cell lines. Molecular docking was furtherly performed to predict the mode of action of the most active synthesized compound **7a** inside the active sites of EGFR and CDK-2. The results of the *invitro* enzyme inhibitory activity, cell cycle analysis, apoptosis and docking studies were perfectly complying with the NCI screening antiproliferative activity results. Furthermore, flow cytometry analysis indicated that compound **7a** arrested the cells at S phase of the cell cycle. Last but not least, all the previously mentioned results proved that the newly synthesized compounds possessed promising antiproliferative activity against renal, breast and ovarian cell lines (UO-31, MCF-7 and IGROV-1), respectively.

Acknowledgments

Great Thanks to the *National Cancer Institute*, for screening the cytotoxic potency of the novel synthesized compounds

Declaration of Competing Interest

- The authors declared that there are no personal relationships that may influence this work.
- The authors declare the following financial interests/personal relationships which may be considered as potential competing interests
-

Credit authorship contribution statement

Eman G. Said: Investigation, Writing–original draft, Visualization **Asmaa A. Mohammed:** Investigation, Methodology, Writing –original draft, Data curation. **Mohammed T. Elsaadi:** Supervision and Conceptualization. **Noha H. Amin:**Conceptualization and writing- editing.

Supplementary data

Supplementary data including all spectral data and copies of IR, Mass, Elemental analyses H_1-NMR, ^{13}C- NMR spectra and NCI screening results of all final compounds were available.

References

[1] Huang L, Fu L. Mechanisms of resistance to EGFR tyrosine kinase inhibitors. Acta. Pharm Sin. B. 2015;(5):390–401. https://doi.org/10.1016/j.apsb.2015.07.001.

[2] Bonanno L, Jirillo A, Favaretto A. Mechanisms of Acquired Resistance to Epidermal Growth Factor Receptor Tyrosine Kinase Inhibitors and New Therapeutic Perspectives in NonSmall Cell Lung Cancer.Curr. Drug Targets. 2011;12 :922–933. http://dx.doi.org/10.2174/138945011795528958

[3] Haider T, Pandey V, Banjare, Gupta PN, Soni V. Drug resistance in cancer: Mechanisms and tackling strategies. Pharmacol. Rep. 2020;72: 1125– 1151. doi: 10.1007/s43440-020-00138-7.

[4] Mansoori B, Mohammadi A, Davudian S, Shirjang S, Baradaran B.the Different Mechanisms of Cancer Drug Resistance: A Brief Review. Adv. Pharm. Bull. 2017;7 :339–348. doi: 10.15171/apb.2017.041

[5] Holohan C, Van Schaeybroeck S, Longley DB, Johnston PG. Cancer drug resistance: An evolving paradigm. Nat. Rev. Cancer 2013; 13: 714–726. doi: 10.1038/nrc3599.

[6] Wang X, Zhang H, Chen X. Drug resistance and combating drug resistance in cancer. Cancer Drug Resist.2019; 2: 141–160 doi: 10.20517/cdr.2019.10.

[7] Zhang XY, Zhang PY. Combinations in multimodality treatments and clinical outcomes during cancer (Review). Oncol. Lett.12016; 2: 4301–4304 https://doi.org/10.3892/ol.2016.5242.

[8] Van Leeuwen RW, Swart EL, Boven E, Boom FA, Schuitenmaker MG, Hugtenburg JG. Potential drug interactions in cancer therapy: a prevalence study using an advanced screening method. Ann. Oncol. 2011; 22 :2334–2341. doi: 10.1093/annonc/mdq761.

[9] Omar HA, Sargeant AM, Wang JR, Wang D, Kulp SK, Patel T, Chen CS. Targeting of the Akt-Nuclear Factor-κB Signaling Network by [1- (4-Chloro-3-nitrobenzenesulfonyl)-1H-indol-3-yl]-methanol (OSU-A9), a Novel Indole-3-Carbinol Derivative, in a Mouse Model of Hepatocellular Carcinoma. Mol. Pharmacol. 2009; 76: 957–968. https://doi.org/10.1124/mol.109.058180

[10] Xie L, Bourne PE. Developing multi-target therapeutics to fine-tune the evolutionary dynamics of the cancer ecosystem. Front. Pharmacol. 2015; 6: 209. https://doi.org/10.3389/fphar.2015.00209

[11] Fu RG, Sun Y, Sheng WB, Liao DF. Designing multi-targeted agents: An emerging anticancer drug discovery paradigm. Eur J Med Chem. 2017;136: 195-211. doi: 10.1016/j.ejmech.2017.05.016. PMID: 28494256.

[12] Wu YW, Chao MW, Tu HJ, Chen LC, Hsu KC, Liou JP, Yang CR, Yen SC, HuangFu WC, Pan SL. A novel dual HDAC and HSP90 inhibitor, MPT0G449, downregulates oncogenic pathways in human acute leukemia in vitro and in vivo. Oncogenesis. 2021; 10 (5):39. doi: 10.1038/s41389- 021-00331-0.

[13] Seymour L. Novel anti-cancer agents in development: exciting prospects and new

challenges. Cancer Treat. Rev. 1999; 25: 301–312. doi: 10.1053/ctrv.1999.0134.

[14] Kamath S and Buolamwini JK. Receptor-Guided Alignment-Based Comparative 3D-QSAR Studies of Benzylidene Malonitrile Tyrphostins as EGFR and HER-2 Kinase Inhibitors. J. Med. Chem. 2003; 46: 4657–4668. doi.org/10.1021/jm030065n.

[15] Meunier B. Hybrid Molecules with a Dual Mode of Action: Dream or Reality? Acc, Chem. Res.2008; 41: 69–77. doi.org/10.1021/ar7000843.

[16] Dallavalle S, Dobri˘ci´c V, Lazzarato L, Machuqueiro E, Pajeva M, Tsakovska I, Zidar I, Fruttero N. Improvement of conventional anti-cancer drugs as new tools against multidrug resistant tumors. Drug Resist. Updates. 2020; 50: 100682-100696. doi: 10.1016/j.drup.2020.100682.

[17] Abdallah T, Ashraf HB, Farag FS, Khaled E, Hamada SA. Unravelling the anticancer potency of 1,2,4-triazole-*N*-arylamide hybrids through inhibition of STAT3: synthesis and in silico mechanistic studies. Molecular diversity.2021; 25:403-420. https ://doi.org/10.1007/s1103 0-020-10131 -0

[18] Ahmed AG, Ahmed ME, Farag FS, Ashraf HB, Kamal ME, Khaied E, Ahmed AA, Rogy RE, Marwa AS, Hamaa SA. Pharmacophore-linked pyrazolo[3,4-*d*] pyrimidines as EGFR-TK inhibitors: Synthesis, anticancer evaluation, pharmacokinetics, and in silico mechanistic studies.ARCH PHARM.2021; e2100258.DOI: 10.1002/ardp.202100258

[19] Khaled, Abdel-Ghany AE, Helmy S, Rezk RA, Hazem AM, Mohamed N, Hamada SA, Sanadelaslam SA. Design, synthesis, molecular docking, anticancer evaluations, and in silico pharmacokinetic studies of novel 5-[(4-chloro/2,4-dichloro) benzylidene] thiazolidine-2,4-dione derivatives as VEGFR-2 inhibitors. ARCH PHARM.2020.https://doi.org/10.1002/ardp.202000279

[20] Karpov OA, Fearnley GW and Smith GA. Receptor tyrosine kinase structure and function in health and disease. AIMS Biophysics. 2015; 2: 476-502. doi: 10.3934/biophy.2015.4.476

[21] Reck M, Zandwijk NV, Gridelli C, et al. Erlotinib in Nonsmall Cell Lung Cancer. Efficacy and Safety Findings of the Global Phase IV Tarceva Lung Cancer Survival Treatment Study. J. Thorac. Oncol. 2010; 5: 1616–1622. doi:10.1097/jT0.0b013e3181f.

[22] Zwick E, Bange J, Ullrich A. Receptor tyrosine kinase signalling as a target for cancer intervention strategies. Endocr. Relat. Cancer. 2001; 8: 161- 173. doi: 10.1677/erc.0.0080161.

[23] Adjei AA. Blocking oncogenic Ras signaling for cancer therapy. Natl. Cancer Inst. 2001; 93: 1062–1074. doi: 10.1093/jnci/93.14.1062.

[24] Druker BJ. STI571 (Gleevec) as a paradigm for cancer therapy, Trends Mol. Med. 2002; 8: S14–S18. doi: 10.1016/s1471-4914(02)02305-5.

[25] Blume-Jesen P and Hunter T. Oncogenic kinase signaling. Nature. 2001; 411: 355–365. doi: 10.1038/35077225.

[26] Ciardiello F and Tortora G. A novel approach in the treatment of cancer: targeting the epidermal growth factor receptor. Clin. Cancer Res. 2001;7: 2958–2970. doi: 10.1158/1078-0432.CCR-04-0870.

[27] Kim H, Yoon Y, Kim J, Han S, Hur H, Park J, Lee J, Oh DY, Im SA, Bang Y, and Kim T. Lapatinib, a Dual EGFR and HER2 Tyrosine Kinase Inhibitor, Downregulates Thymidylate Synthase by Inhibiting the Nuclear Translocation of EGFR and HER2. PLoS ONE. 2009; 4:1-9. doi: 10.1371/journal.pone.0005933

[28] Pavletich NP. Mechanisms of cyclin-dependent kinase regulation: structures of Cdks, their cyclin activators, and Cip and INK4 inhibitors. Mol. Biol. 1999; 287: 821-828. doi: 10.1006/jmbi.1999.2640.

[29] Keaton, Mignon A. “Morgan DO: The Cell Cycle: Principles of Control (Primers in Biology).” Cell Division. 2007; 2: 1-2. doi:10.1186/1747-1028-2- 27

[30] Osuga H, Osuga S, Wang F, Fetni R, Hogan MJ, Slack RS, Hakim AM, Ikeda JE, Park DS. Oxidative Stress and Neurodegenerative Disorders. Natl. Acad. Sci. USA. 2000; 97: 10254–10259.

[31] Sielecki TM, Johnson TL, Liu J, Muckelbauer JK, Grafstrom, RH, Cox S, Boylan JF, Burton CR, Chen HL, Smallwood AM, Chang CH, Boisclair MD, Benfield PA, Trainor GL, & Seitz SP. “Quinazolines as cyclin dependent kinase inhibitors.” Bioorg. Med. Chem. Letters. 2001; (11) 9 :1157-1160. https://doi.org/10.1016/S0960- 894X (01)00185-8

[32] Shewchuk L, Hassell A, Wisely B, Rocque W, Holmes W, Veal J & Kuyper LF. Binding mode of the 4-anilinoquinazoline class of protein kinase inhibitor: X-ray crystallographic studies of 4-anilinoquinazolines bound to cyclin-dependent kinase 2 and p38 kinase. J. Med.

Chem. 2000; 43:133–138 https://doi.org/10.1021/jm990401t

[33] Eman RM & Ghada FE. Development of newly synthesised quinazolinone-based CDK2 inhibitors with potent efficacy against melanoma. Journal of Enzyme Inhibition and Medicinal Chemistry. 2022; 37(1): 686-700. doi: 10.1080/14756366.2022.2036985

[34] Carreras CW, Santi DV. The catalytic mechanism and structure of thymidylate synthase. Annu. Rev. Biochem. 1995; 64: 721-762. doi: 10.1146/annurev.bi.64.070195.003445.

[35] Roukos DH, Katsios C, Liakakos T. Genotype-phenotype map and molecularnetworks: a promising solution in overcoming colorectal cancer resistance to targeted treatment. Expert Rev. Mol. Diagn. 2010; 10 :541–545. doi: 10.1586/erm.10.49.

[36] Peters GJ, Backus HHJ, Freemantle S, Van Triest B, Codacci-Pisanelli G, Van der Wilt CI, Smid K, Lunec J, Calvert AH, Marsh S, Mcleod HL, Bloemena E, Meijer S, Jansen G, Van Groeningen CJ, Pinedo HM. Induction of thymidylate synthase as a 5-fluorouracil resistance mechanism, Biochim. BiophysActa.Mol. Basis Dis. 2002; 1587 :194–205. doi.org/10.1016/S0925-4439(02)00082-0

[37] Fujii R, Seshimo A, Kameoka S. Relationships between the expression of thymidylate synthase, dihydropyrimidine dehydrogenase, and orotate phosphoribosyltransferase and cell proliferative activity and 5-fluorouracil sensitivity in colorectal carcinoma. Int J Clin Oncol. 2003; 8: 72- 78. doi: 10.1007/s101470300013.

[38] Milik SN, Lasheen DS, Serya RAT, Abouzid KAM. How to train your inhibitor:Design strategies to overcome resistance to epidermal growth factor receptor inhibitors . Eur. J. Med. Chem. 2017; 142: 131–151. doi: 10.1016/j.ejmech.2017.07.023.

[39] Berman EM, Werbel LM.The renewed potential for folate antagonists in contemporary cancer chemotherapy.J. Med. Chem. 1991;34 :479–485. doi: 10.1021/jm00106a001.

[40] Clark JL, Berger SL, Mittelman A, Berger FG. Thymidylate synthase gene amplification in a colon tumor resistant to fluoropyrimidine chemotherapy.Cancer Treat Rep. 1987; 71: 261-265.

[41] Swain SM, Lippman ME, Egan EF, Drake JC, Steinberg SM, Allegra CJ. Fluorouracil and high-dose leucovorin in previously treated patients with metastatic breast cancer. J Clin Oncol.1989; 7: 890-899. doi: 10.1200/JCO.1989.7.7.890.

[42] Ichikawa W, Uetake H, Shirota Y, Yamada H, Nishi N, Nihei Z, Sugihara K, Hirayama R. Combination of dihydropyrimidine dehydrogenase and thymidylate synthase gene expressions in primary tumors as predictive parameters for the efficacy of fluoropyrimidine-based chemotherapy for metastatic colorectal cancer. Clin Cancer Res.2003; 9 :786–791.

[43] Ai T, Cui H, Chen L. Multi-targeted histone deacetylase inhibitors in cancer therapy. Curr. Med. Chem. 2012; 19: 475–487. doi: 10.2174/092986712798918842.

[44] Gediva LK, Njar VCO. Promise and challenges in drug discovery and development of hybrid anticancer drugs Expert Opin, Drug Discov. 2009; 4: 1099–1111.

[45] El-Naggar AM, Abou-El-Regal MM, El-Metwally SA, Sherbiny FF, Eissa IH. Synthesis, characterization and molecular docking studies of thiouracil derivatives as potent thymidylate synthase inhibitors and potential anticancer agents. Mol. Divers. 2017; 21 :967–983. https://doi.org/10.1007/s11030-017-9776-1.

[46] Abdellatif KRA, Belal A, El-Saadi MT, Amin NH, Said EG, Hemeda LR. Design, synthesis, molecular docking and antiproliferative activity of some novel benzothiazole derivatives targeting EGFR/HER2 and TS. Bioorg.Chem.2020; 101: 103976-103997. doi: 10.1016/j.bioorg.2020.103976.

[47]Al-Salahi R, Marzouk M, Ashour AE, Alswaidan I. Synthesis and Antitumor Activity of 1,2,4-Triazolo[1,5-a]-Quinazolines. Asian J. Chem. 2014; 26: 2173–2176, DOI:10.14233/ajchem.2014.16849.

[48] Akash Jori J, Sheshagiri RD and Gurubasavraj VP. synthesis and in vitro Cytotoxicity Study of Novel 4-Substituted Quinazolines Encompassed with Thiazolidinone and Azetidinone. Asian J. Chem.2020; 32(10): 2617-2623 https://doi.org/10.14233/ajchem.2020.22837

[49] Kovalenko IS et al. Synthesis and anticancer activity of 2-(alkyl-, alkaryl-, aryl-, hetaryl-[1,2, 4]triazolo[1,5-c]quinazolines. Sci Pharm. 2013; 81(2): 359-391. doi:10.3797/scipharm.1211-08

[50] Kambe S, Saito K, Kishi H, Sakurai A and Midorikawa HA. one- step synthesis of 4-oxo-2-thioxopyrimidine derivatives by the ternary condensation of ethyl cyanoacetate,

aldehydes, and thiourea. Synthesis. 1979; 4: 287-289. doi:10.1055/s-1979-28650.

[51] Alley MC, Scudiero DA, Mons A, Hursey ML, Czerwinski MJ, Fine DL, Abbott BJ, Mayo A, Shoemaker RH, Boyd MR. Feasibility of drug screening with panels of human tumor cell lines using a microculture tetrazolium assay, cancer Res. 1988; 48: 589-601,

[52] Anne M, Dominic S, Philip S, Robert S, Kenneth P, David V, Curtis H, John L, Paul C, Anne V, Marcia G, Hugh C, Joseph M, Michael B.Feasibility of a High-Flux Anticancer Drug Screen Using a Diverse Panel of Cultured Human Tumor Cell Lines. Journal of the National Cancer Institute.1991; 83:757-766 https://doi.org/10.1093/jnci/83.11.757

[53] Abdelhafez OM, Ahmed EY, Latif NA, Arafa RK, Elmageed ZY, Ali HI. Design and molecular modeling of novel P38α MAPK inhibitors targeting breast cancer, synthesized from oxygen heterocyclic natural compounds. Bioorg. Med. Chem. (2019); 27: 1308–1319. doi: 10.1016/j.bmc.2019.02.027.

[54] Kassab AE, Hassan RA. Novel benzotriazole N-cylarylhydrazone hybrids: Design, synthesis, anticancer activity, effects on cell cycle profile, caspase-3 mediated apoptosis and FAK inhibition, Bioorg Chem. 2018; 80: 531–544, doi: 10.1016/j.bioorg.2018.07.008.

[55] Mokhtar AM, El-Messery SM, Ghaly MA, Hassan GS. Targeting EGFR tyrosine kinase: Synthesis, in vitro antitumor evaluation, and molecular modeling studies of benzothiazole-based derivatives. Bioorg. Chem. 2020; 104: 104259-104275. doi: 10.1016/j.bioorg.2020.104259